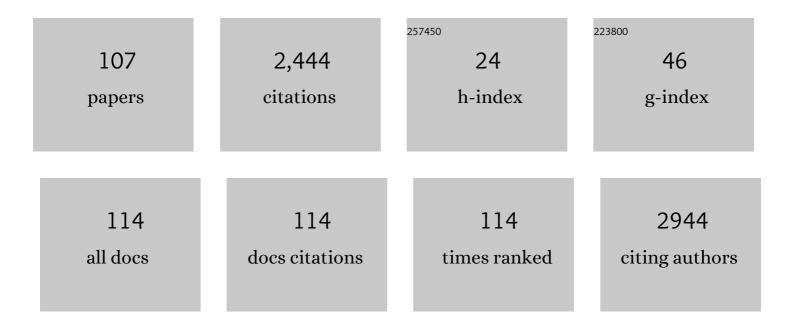
List of Publications by Year in descending order

Source: https://exaly.com/author-pdf/6526821/publications.pdf Version: 2024-02-01



#	Article	IF	CITATIONS
1	The 2010 explosive eruption of Java's Merapi volcano—A â€~100-year' event. Journal of Volcanology and Geothermal Research, 2012, 241-242, 121-135.	2.1	336
2	Finite fault inversion of DInSAR coseismic displacement of the 2009 L'Aquila earthquake (central Italy). Geophysical Research Letters, 2009, 36, .	4.0	258
3	Satellite radar and optical remote sensing for earthquake damage detection: results from different case studies. International Journal of Remote Sensing, 2006, 27, 4433-4447.	2.9	177
4	Geodetic model of the 2016 Central Italy earthquake sequence inferred from InSAR and GPS data. Geophysical Research Letters, 2017, 44, 6778-6787.	4.0	162
5	Soil moisture estimation over vegetated terrains using multitemporal remote sensing data. Remote Sensing of Environment, 2010, 114, 440-448.	11.0	107
6	Earthquake Damages Rapid Mapping by Satellite Remote Sensing Data: L'Aquila April 6th, 2009 Event. IEEE Journal of Selected Topics in Applied Earth Observations and Remote Sensing, 2011, 4, 935-943.	4.9	56
7	Uplift and subsidence due to the 26 December 2004 Indonesian earthquake detected by SAR data. International Journal of Remote Sensing, 2008, 29, 3891-3910.	2.9	54
8	Analysis of satellite and in situ ground deformation data integrated by the SISTEM approach: The April 3, 2010 earthquake along the Pernicana fault (Mt. Etna - Italy) case study. Earth and Planetary Science Letters, 2011, 312, 327-336.	4.4	52
9	Earthquake damage mapping: An overall assessment of ground surveys and VHR image change detection after L'Aquila 2009 earthquake. Remote Sensing of Environment, 2018, 210, 166-178.	11.0	51
10	New insights into earthquake precursors from InSAR. Scientific Reports, 2017, 7, 12035.	3.3	46
11	Land subsidence, Ground Fissures and Buried Faults: InSAR Monitoring of Ciudad GuzmÃin (Jalisco,) Tj ETQq1 1 (	0.784314 4.0	rgBT /Overloo
12	X-, C-, and L-Band DInSAR Investigation of the April 6, 2009, Abruzzi Earthquake. IEEE Geoscience and Remote Sensing Letters, 2011, 8, 49-53.	3.1	42
13	Coseismic slip distribution for the <i>M<sub>w</sub></i> 9 2011 Tohokuâ€Oki earthquake derived from 3â€Ð FE modeling. Journal of Geophysical Research: Solid Earth, 2013, 118, 3837-3847.	3.4	38
14	Pyroclastic density current volume estimation after the 2010 Merapi volcano eruption using X-band SAR. Journal of Volcanology and Geothermal Research, 2013, 261, 236-243.	2.1	37
15	The Campotosto Seismic Gap in Between the 2009 and 2016–2017 Seismic Sequences of Central Italy and the Role of Inherited Lithospheric Faults in Regional Seismotectonic Settings. Tectonics, 2018, 37, 2425-2445.	2.8	37
16	Monitoring Soil Moisture in an Agricultural Test Site Using SAR Data: Design and Test of a Pre-Operational Procedure. IEEE Journal of Selected Topics in Applied Earth Observations and Remote Sensing, 2013, 6, 1199-1210.	4.9	34
17	The May 12, 2008, (Mw 7.9) Sichuan Earthquake (China): Multiframe ALOS-PALSAR DInSAR Analysis of Coseismic Deformation. IEEE Geoscience and Remote Sensing Letters, 2010, 7, 266-270.	3.1	32
18	Multisensor Satellite Monitoring of the 2011 Puyehue-Cordon Caulle Eruption. IEEE Journal of Selected Topics in Applied Earth Observations and Remote Sensing, 2014, 7, 2786-2796.	4.9	31

#	Article	IF	CITATIONS
19	Volume unbalance on the 2016 Amatrice - Norcia (Central Italy) seismic sequence and insights on normal fault earthquake mechanism. Scientific Reports, 2019, 9, 4250.	3.3	29
20	20 years of active deformation on volcano caldera: Joint analysis of InSAR and AInSAR techniques. International Journal of Applied Earth Observation and Geoinformation, 2013, 23, 279-287.	2.8	27
21	Monthly migration of a tectonic seismic swarm detected by DInSAR: southwest Peloponnese, Greece. Geophysical Journal International, 2013, 194, 1302-1309.	2.4	27
22	A method for multi-hazard mapping in poorly known volcanic areas: an example from Kanlaon (Philippines). Natural Hazards and Earth System Sciences, 2013, 13, 1929-1943.	3.6	27
23	Using multi-band InSAR data for detecting local deformation phenomena induced by the 2016–2017 Central Italy seismic sequence. Remote Sensing of Environment, 2017, 201, 234-242.	11.0	27
24	Relative Sea-Level Rise Scenario for 2100 along the Coast of South Eastern Sicily (Italy) by InSAR Data, Satellite Images and High-Resolution Topography. Remote Sensing, 2021, 13, 1108.	4.0	26
25	Ground Deformation and Source Geometry of the 30 October 2016 Mw 6.5 Norcia Earthquake (Central) Tj ETQq1 Remote Sensing, 2018, 10, 1901.	1 0.7843 4.0	14 rgBT /0v 25
26	Did the September 2010 (Darfield) earthquake trigger the February 2011 (Christchurch) event?. Scientific Reports, 2011, 1, 98.	3.3	24
27	The seismic sequence of January–February 2014 at Cephalonia Island (Greece): constraints from SAR interferometry and GPS. Geophysical Journal International, 2015, 203, 1528-1540.	2.4	24
28	Coseismic liquefaction phenomenon analysis by COSMO-SkyMed: 2012 Emilia (Italy) earthquake. International Journal of Applied Earth Observation and Geoinformation, 2015, 39, 65-78.	2.8	24
29	Did Anthropogenic Activities Trigger the 3 April 2017 Mw 6.5 Botswana Earthquake?. Remote Sensing, 2017, 9, 1028.	4.0	23
30	The Causative Fault of the 2016 Mwp 6.1 Petermann Ranges Intraplate Earthquake (Central Australia) Retrieved by C- and L-Band InSAR Data. Remote Sensing, 2018, 10, 1311.	4.0	21
31	Heterogeneous Behavior of the Campotosto Normal Fault (Central Italy) Imaged by InSAR GPS and Strong-Motion Data: Insights from the 18 January 2017 Events. Remote Sensing, 2019, 11, 1482.	4.0	21
32	The Interferometric Use of Radar Sensors for the Urban Monitoring of Structural Vibrations and Surface Displacements. IEEE Journal of Selected Topics in Applied Earth Observations and Remote Sensing, 2016, 9, 3761-3776.	4.9	19
33	Coseismic deformation pattern of the Emilia 2012 seismic sequence imaged by Radarsat-1 interferometry. Annals of Geophysics, 2012, 55, .	1.0	19
34	Aftershocks, groundwater changes and postseismic ground displacements related to pore pressure gradients: Insights from the 2012 Emiliaâ€Romagna earthquake. Journal of Geophysical Research: Solid Earth, 2017, 122, 5622-5638.	3.4	18
35	The Relationship between InSAR Coseismic Deformation and Earthquake-Induced Landslides Associated with the 2017 Mw 3.9 Ischia (Italy) Earthquake. Geosciences (Switzerland), 2018, 8, 303.	2.2	18
36	InSAR Monitoring of Italian Coastline Revealing Natural and Anthropogenic Ground Deformation Phenomena and Future Perspectives. Sustainability, 2018, 10, 3152.	3.2	18

#	Article	IF	CITATIONS
37	Intercomparison and Validation of SAR-Based Ice Velocity Measurement Techniques within the Greenland Ice Sheet CCI Project. Remote Sensing, 2018, 10, 929.	4.0	18
38	The 24 August 2016 Amatrice earthquake: macroseismic survey in the damage area and EMS intensity assessment. Annals of Geophysics, 2016, 59, .	1.0	18
39	Combined use of ground-based systems for Cultural Heritage conservation monitoring. , 2014, , .		17
40	Earthquake damage mapping by using remotely sensed data: the Haiti case study. Journal of Applied Remote Sensing, 2017, 11, 016042.	1.3	16
41	Ground Deformation Imagery of the May Sichuan Earthquake. Eos, 2008, 89, 341-342.	0.1	15
42	High-precision levelling, DInSAR and geomorphological effects in the Emilia 2012 epicentral area. Geomorphology, 2015, 235, 106-117.	2.6	15
43	X- and C-Band SAR Surface Displacement for the 2013 <i>Lunigiana</i> Earthquake (Northern Italy): A Breached Relay Ramp?. IEEE Journal of Selected Topics in Applied Earth Observations and Remote Sensing, 2014, 7, 2746-2753.	4.9	14
44	An innovative procedure for monitoring the change in soil seismic response by InSAR data: application to the Mexico City subsidence. International Journal of Applied Earth Observation and Geoinformation, 2016, 53, 146-158.	2.8	14
45	Synergic Use of Multi-Sensor Satellite Data for Volcanic Hazards Monitoring: The Fogo (Cape Verde) 2014–2015 Effusive Eruption. Frontiers in Earth Science, 2020, 8, .	1.8	14
46	Uncovering deformation processes from surface displacements. Journal of Geodynamics, 2016, 102, 58-82.	1.6	13
47	Step-like displacements of a deep seated gravitational slope deformation observed during the 2016–2017 seismic events in Central Italy. Engineering Geology, 2018, 246, 337-348.	6.3	13
48	Aftershock Rate and Pore Fluid Diffusion: Insights From the Amatriceâ€Vissoâ€Norcia (Italy) 2016 Seismic Sequence. Journal of Geophysical Research: Solid Earth, 2019, 124, 995-1015.	3.4	13
49	Gravity-driven postseismic deformation following the Mw 6.3 2009 L'Aquila (Italy) earthquake. Scientific Reports, 2015, 5, 16558.	3.3	12
50	The epicentral fingerprint of earthquakes marks the coseismically activated crustal volume. Earth-Science Reviews, 2021, 218, 103667.	9.1	12
51	Are normal fault earthquakes due to elastic rebound or gravitational collapse?. Annals of Geophysics, 2020, 63, .	1.0	11
52	The Calibration of the Envisat Radar Altimeter Receiver by a Passive Technique. IEEE Transactions on Geoscience and Remote Sensing, 2006, 44, 3297-3307.	6.3	10
53	A Multidisciplinary Study of the DPRK Nuclear Tests. Pure and Applied Geophysics, 2014, 171, 341-359.	1.9	10
54	Triple Collocation to Assess Classification Accuracy Without a Ground Truth in Case of Earthquake Damage Assessment. IEEE Transactions on Geoscience and Remote Sensing, 2018, 56, 485-496.	6.3	9

#	Article	IF	CITATIONS
55	SAR and Optical Data Comparison for Detecting Co-Seismic Slip and Induced Phenomena during the 2018 Mw 7.5 Sulawesi Earthquake. Sensors, 2019, 19, 3976.	3.8	9
56	Lithological control on multiple surface ruptures during the 2016–2017 Amatrice-Norcia seismic sequence. Journal of Geodynamics, 2020, 134, 101676.	1.6	9
57	Multi-polarization C-band SAR imagery to quantify damage levels due to the Central Italy earthquake. International Journal of Remote Sensing, 2021, 42, 5969-5984.	2.9	9
58	Analysis of a large seismically induced mass movement after the December 2018 Etna volcano (southern Italy) seismic swarm. Remote Sensing of Environment, 2021, 263, 112524.	11.0	9
59	Geohazards Monitoring and Assessment Using Multi-Source Earth Observation Techniques. Remote Sensing, 2021, 13, 4269.	4.0	9
60	Transponder calibration of the Envisat RA-2 altimeter Ku band sigma naught. Advances in Space Research, 2013, 51, 1478-1491.	2.6	8
61	An improved data integration algorithm to constrain the 3D displacement field induced by fast deformation phenomena tested on the Napa Valley earthquake. Computers and Geosciences, 2017, 109, 206-215.	4.2	8
62	A New Damage Assessment Method by Means of Neural Network and Multi-Sensor Satellite Data. Applied Sciences (Switzerland), 2017, 7, 781.	2.5	8
63	Minimum Redundancy Array—A Baseline Optimization Strategy for Urban SAR Tomography. Remote Sensing, 2020, 12, 3100.	4.0	8
64	Three-dimensional numerical simulation of the interseismic and coseismic phases associated with the 6 April 2009, Mw 6.3ÂL'Aquila earthquake (Central Italy). Tectonophysics, 2021, 798, 228685.	2.2	8
65	Numerical analysis of interseismic, coseismic and post-seismic phases for normal and reverse faulting earthquakes in Italy. Geophysical Journal International, 2021, 225, 627-645.	2.4	8
66	Source identification for situational awareness of August 24th 2016 Central Italy event. Annals of Geophysics, 2016, 59, .	1.0	7
67	Comparing and combining the capability of detecting earthquake damages in urban areas using SAR and optical data. , 0, , .		6
68	Automatic damage detection Using pulse-coupled neural networks For the 2009 Italian earthquake. , 2010, , .		6
69	Objects textural features sensitivity for earthquake damage mapping. , 2011, , .		6
70	Quickbird Panchromatic Images for Mapping Damage at Building Scale Caused by the 2003 Bam Earthquake. , 2008, , .		5
71	The SIGRIS Project: A Remote Sensing System for Seismic Risk Management. , 2008, , .		5
72	Synthetic Aperture Radar (SAR) Doppler Anomaly Detected During the 2010 Merapi (Java, Indonesia) Eruption. IEEE Geoscience and Remote Sensing Letters, 2013, 10, 1319-1323.	3.1	5

CHRISTIAN BIGNAMI

#	Article	IF	CITATIONS
73	Exploitation of Copernicus Sentinels Data for Sensing Fire-Disturbed Vegetated Areas. , 2018, , .		5
74	Transponder calibration of the ENVISAT RA-2 altimeter sigma naught. , 2012, , .		4
75	Identification of building double-bounces feature in very high resoultion SAR data for earthquake damage mapping. , 2015, , .		4
76	SAR and optical remote sensing for urban damage detection and mapping: case studies. , 2007, , .		3
77	Using Multi-Frequency Insar Data to Constrain Ground Deformation of Ischia Earthquake. , 2018, , .		3
78	Precise Topographic Model Assisted Slope Displacement Retrieval from Small Baseline Subsets Results: Case Study over a High and Steep Mining Slope. Sensors, 2020, 20, 6674.	3.8	3
79	High resolution mapping of soil moisture by SAR: Data integration and exploitation of prior information. , 2009, , .		2
80	Towards an operational procedure to map soil moisture using SAR: Results of a seven-year-experiment over an agricultural area. , 2011, , .		2
81	Volcanic product detection after the 2010 Merapi eruption by using VHR SAR data. , 2012, , .		2
82	New results on post-seismic deformations over L'Aquila, Italy, by high resolution PSP SAR interferometry. , 2013, , .		2
83	Classification of VHR optical data for land use change analysis by scale object seletion (SOS) algorithm. , 2014, , .		2
84	Detecting earthquake damage in urban area: application to COSMO-SkyMed imagery of L'Aquila earthquake. Proceedings of SPIE, 2015, , .	0.8	2
85	Multi-sensor monitoring of Ciudad Guzman (Mexico) ground subsidence. Procedia Computer Science, 2018, 138, 362-365.	2.0	2
86	Earthquake Source Investigation of the Kanallaki, March 2020 Sequence (North-Western Greece) Based on Seismic and Geodetic Data. Remote Sensing, 2021, 13, 1752.	4.0	2
87	A multisensor approach for the 2016 Amatrice earthquake damage assessment. Annals of Geophysics, 2016, 59, .	1.0	2
88	Exploiting Physical and Topographic Information within a Fuzzy Scheme to Map Flooded Area by SAR. , 2006, , .		1
89	Neural Networks for automatic seismic source analysis from DInSAR data. , 2011, , .		1
90	The Intraplate 2016 Mw 6.0 Australia Earthquake Studied by Insar Data. , 2018, , .		1

6

#	Article	IF	CITATIONS
91	Multi-Hazard Analysis of Etna 2018 Eruption by Sar Imaging. , 2019, , .		1
92	Cosesimic liquefaction phenomena from DInSAR after the May 20, 2012 Emilia earthquake. Rendiconti Online Societa Geologica Italiana, 0, 35, 5-9.	0.3	1
93	Retrieval and analysis of land surface microwave emissivity from SSM/I data. European Journal of Remote Sensing, 2008, , 15-25.	0.2	1
94	Preliminary results on soil moisture mapping in alessandria area (northern Italy) using Envisat A-SAR. , 0, , .		0
95	Microwave Signature of the Greenland Ice Sheet at Ku- and S-Bands. IEEE Geoscience and Remote Sensing Letters, 2009, 6, 322-326.	3.1	0
96	Joint inversion of the 2011 Tohoku (Japan) earthquake from dinsar and GPS data. , 2012, , .		0
97	DInSAR techniques for studying the October 23, 2011, Van earthquake (Turkey), and its relationship with neighboring structures. , 2012, , .		0
98	Comment on "Surface deformation caused by April 6th 2009 earthquake in L'Aquila (Italy): A comparative analysis from ENVISAT ASAR, ALOS PALSAR and ASTER―by M.A. Goudarzi, T. Woldai, V.A. Tolpekin. International Journal of Applied Earth Observation and Geoinformation, 2012, 18, 579-581.	2.8	0
99	A possibile breached relay ramp causing the 2013 Lunigiana earthquake (Northern Italy). , 2014, , .		0
100	Detecting sparse earthquake damages in high density urban settlements by VHR SAR data. , 2014, , .		0
101	Lava emplacement mapping with SAR and optical satellite data. , 2017, , .		0
102	Atmospheric Slant Delay from SAR Interferometry, GNSS and Numerical Weather Prediction Model: A Comparison Study in View of a Geosynchronous SAR Mission. , 2018, , .		0
103	The Co-Seismic Slip Induced By the 2018 Sulawesi Earthquake on Palu Bay Imaged By Sar and Optical Data. , 2019, , .		0
104	Earthquake Damage Assessment Using C-Band Polsar Measurements and Ground Surveys. , 2021, , .		0
105	Earthquake Damage Assessment from VHR Data: Case Studies. , 2015, , 630-637.		0
106	Advanced procedures for volcanic and seismic monitoring. International Journal of Safety and Security Engineering, 2016, 6, 114-121.	1.0	0
107	Exploitation of SAR data to detect burned areas in the Sila mountain area (southern Italy). , 2018, , .		0